

Can COBE see the shape of the universe?

Neil J. Cornish^y, David Spergel^z and Glenn Starkman^z^yRelativity Group, DAMTP, Cambridge University, Silver Street, Cambridge CB3 9EW, England^zDepartment of Astrophysical Sciences, Princeton University, Princeton, New Jersey 08544^zDepartment of Physics, Case Western Reserve University, Cleveland, Ohio 44106-7079

In recent years, the large angle COBE (DMR) data has been used to place constraints on the size and shape of certain topologically compact models of the universe. Here we show that this approach does not work for generic compact models. In particular, we show that compact hyperbolic models do not suffer the same loss of large angle power seen in flat or spherical models. This follows from applying a topological theorem to show that generic hyperbolic three manifolds support long wavelength fluctuations, and by taking into account the dominant role played by the integrated Sachs-Wolfe effect in a hyperbolic universe.

98.70.Vc, 98.80.Cq, 98.80.Hw

In 1966, Marc Kac [1] posed the question 'Can one hear the shape of a drum?'. In recent years a similar question has been asked in cosmology; 'Can one see the shape of the universe?' [2]. More formally, the question can be phrased: can we discern the global topology of the universe by studying fluctuations in the cosmic microwave background radiation (CMB)?

With the launch of new satellites next century, and with a careful search for matched microwave temperatures around pairs of circles on the last scattering surface ('topological lensing') [3,4], we should be able to answer this question in the affirmative. In the interim, we can ask how much can be done with the 4-year COBE (DMR) data [5]. Poor angular resolution and low signal to noise make the COBE data unsuitable for direct lensing studies, but several groups [6,7,8,9,10] have used the data to put constraints on a variety of toroidal models. Here we consider how their results might be generalised to encompass a wider class of small universe models. In particular we will be interested in hyperbolic models since observations suggest we live in a negatively curved universe. Moreover, the topology scale and the curvature scale are intimately related in hyperbolic models, whereas in flat universes there is no scale at which one would expect to observe the topology. By applying a number of results pertaining to the topology of three manifolds, and by taking into account the integrated Sachs-Wolfe effect, we show that generic small universe models cannot be constrained by COBE data.

Small universes enjoy the same local geometry and dynamics as the usual simply connected FRW models^y, but display different global characteristics. In particu-

lar, small universes have a discrete spectrum of eigenmodes and are globally anisotropic and inhomogeneous. In models with locally spherical or Euclidean geometry the eigenvalue spectrum is raised above that of the simply connected models and there is a corresponding long wavelength cut-off. Assuming that temperature fluctuations in the CMB are caused by density fluctuations on the last scattering surface, this long wavelength cut-off is translated into a suppression of large angle power [6,7]. The cut-off in long wavelength power that occurs in Euclidean space was first used by Sokolov [6] to show that a flat universe with toroidal spatial sections could not be much smaller than the horizon size. He argued that the topology scale had to be large enough to allow the wavelengths needed to produce the quadrupole anisotropy measured by COBE. A number of groups [7,8,9] have since improved on Sokolov's bound and extended his analysis to include other flat topologies. Recently, Levin et al. [10] have generalised these bounds to include a non-compact, infinite volume hyperbolic topology describing a toroidal horn.

There has been a tendency to draw general conclusions from these few examples. Indeed, the small universe idea was declared dead in Ref. [8]. While it is fair to say that positively curved small universes, and the simplest toroidal flat universes with topology scale much less than the horizon scale are effectively ruled out [9], we show that the same cannot be said about negatively-curved models. Lessons learned in flat space do not always apply in hyperbolic space. For example, the eigenvalue spectrum is typically lowered, rather than raised by making hyperbolic space compact. Consequently, there need not be a long wavelength cut-off. Even if there were, and even assuming a simple initial power spectrum at large wavelengths, the existence of large angle power as measured by COBE (DMR) still could not directly be used to constrain compact hyperbolic models since the large angle power in a negatively curved universe does not come from the last scattering surface. The bulk of the large angle power is due to the decay of curvature perturba-

^yA small universe is defined to be one that is multiply-connected on scales smaller than the horizon.

^yBy simply connected we mean the fundamental group $\pi_1(\mathcal{M})$ is trivial. Since $\pi_1(S^3) = \pi_1(E^3) = \pi_1(H^3) = \mathbb{Z}$, the usual FRW models are all simply connected. A multiply-connected model has a non-trivial fundamental group.

tions along the line of sight [11]. If the universe is hyperbolic, COBE has been detecting fluctuations produced at moderate redshifts $z \approx 1$, rather than $z \approx 1200$. Consequently, the large angle power is produced by fluctuations occurring on small comoving length scales that only appear large due to their relatively close proximity.

In section I we briefly discuss constraints on small universe models based on searches for ghost images. In section II we emphasise the importance of the ISW effect for calculating CMB fluctuations on large angular scales. In section III we describe the eigenmodes of infinite hyperbolic space. In section IV we obtain lower limits on the wavelength of the longest wavelength mode, showing that supercurvature modes always exist, though in what multiplicity we cannot say. In section V we digress to consider a particular class of topologies closely related to the horn topology studied by Levin et al. [10]. In section VI we discuss the method of images as an approach for calculating eigenfunctions on compact hyperbolic manifolds, and identify some of the difficulties. In section VII we discuss the connection between the method of images and quantum chaos, discuss how one might go about exploiting this connection, and some of the obstacles. Our conclusions can be found in section VIII. A glossary of mathematical terms is included in the appendix.

Throughout the paper we will be assuming that a cosmological constant does not provide a significant contribution to the density of the universe.



I. GHOST HUNTING



The most obvious observational signature of a multiply connected universe would be repeated or 'ghost' images of familiar objects such as galaxies or rich clusters [12]. However, searches for ghost images are hampered by evolution of the objects; our ability to recognise objects when viewed from different directions; and the difficulty in determining the distances to objects.

Despite these problems, the consensus seems to be that there is no evidence for ghost images out to redshifts of $z \approx 0.4$ (the current depth of wide-field redshift surveys). It is interesting to note that this lack of ghost images is exactly what one expects for typical small compact hyperbolic models. According to Thurston [13], the expectation value for the length of the shortest closed geodesics in a typical small hyperbolic universe is roughly $(0.5 \pm 1.0)R_0$, where R_0 is the comoving curvature radius. This means that the first copies of the Milky Way galaxy or even a cluster would not be seen before a conformal lookback time of $\approx 0.5 \pm 1.0$. Converting this to redshift space via the relation

$$1 + z = \frac{2(\sqrt{1 - \frac{1}{z}} - 1)}{\cosh(\sqrt{1 - \frac{1}{z}})}; \quad (1.1)$$

where $\eta = \text{arccosh}(2 - \sqrt{1 - \frac{1}{z}})$ is the present conformal time, we find that the first ghost images will be at a

redshift of $z \approx 0.9 \pm 2.9$ in a universe with $\eta_0 = 0.3$. If the universe has η_0 closer to unity, the first ghost images will be even more distant.

These numbers suggest that direct searches for ghost images of astrophysical objects will be unable to tell if we live in a compact hyperbolic universe. A more promising approach is to look for topological lensing of the last scattering surface by studying fluctuations in the cosmic microwave background radiation [3,4].

II. MICROWAVE BACKGROUND FLUCTUATIONS

Standard folklore holds that the finite size of a small universe will lead to a long wavelength cut-off in the spectrum of primordial fluctuations. In the following section we show that this is not true in a hyperbolic universe. Here we point out that even if there were such a cut-off, it could not be detected on the angular scales probed by COBE.

In adiabatic models (e.g. inflation) the primordial fluctuation spectrum determines the power spectrum on the last scattering surface. However, the fluctuations measured by COBE do not necessarily originate on the last scattering surface. In a negatively curved universe, power on angular scales larger than the curvature scale is produced at relatively low redshifts by fluctuations occurring on scales considerably smaller than the curvature scale. This severely limits COBE's ability to probe the large scale topology of the universe.

In a hyperbolic universe, there are two terms that produce the microwave background fluctuations on large angular scales:

$$\frac{T(z)}{T} = \frac{(\chi_{\text{LSS}}; \eta_{\text{LSS}})}{3} + 2 \frac{z}{\eta_{\text{LSS}}} - (\chi; \eta) d; \quad (2.1)$$

where η_{LSS} is the conformal time at the surface of last scatter and η_0 is the present conformal time. The first term is due to variations in the gravitational potential and photon density at the surface of last scatter. The latter term, which is zero to linear order in a matter dominated universe, is due to the decay of potential fluctuations at late times, $(1 + z) < \eta_0^{-1}$. In a universe with $\eta_0 = 0.3$, the latter term, the so-called integrated Sachs-Wolfe effect, is the dominant source of microwave background fluctuations on large angular scales [11]. The late-time ISW effect dominates multipole moments below $\ell_{\text{curv}} = 2\sqrt{1 - \eta_0} = 0$. Neglecting this contribution will lead to a severe underestimate of the large angle power.

Because of the late-time ISW effects, we expect significant large angular scale fluctuations even if η_0 is as small as 0.1. Kamionkowski & Spergel [11] calculated the CMB fluctuations in hyperbolic models with trivial topology and a variety of primordial power spectra. Below the curvature scale the standard scale-invariant

Harrison-Zeldovich spectrum was used. This is probably reasonable at sufficiently small scales for models with non-trivial topology, including compact models, as small scale perturbations will be less sensitive to global properties such as the curvature and topology. Beyond the curvature scale, both the unknown form of the eigenmodes and the expected effects of transients in the inflationary dynamics make the situation much less clear. For the latter reason, Kamionkowski & Spergel considered a range of power spectra. The most conservative model, the "volume power law model", effectively removes all supercurvature fluctuations as it leads to an exponential suppression of supercurvature modes. In this model there is essentially no contribution to $T = T$ from the last scattering surface. Nevertheless, the second term in (2.1) produced sufficient power to fit the fluctuations observed by COBE (see figures 6 and 9 in [11]).

III. VIBRATIONS IN A HYPERBOLIC CAVITY

When attempting to calculate perturbation spectra in compact hyperbolic space one is immediately confronted by the highly non-trivial task of finding the eigenmodes. In principle the eigenmodes of a compact space can be obtained from the eigenmodes of the simply connected covering space using the method of images [14]. In practice the sums involved are highly divergent and can only be tamed by sophisticated resummation methods [15,16]. Before confronting this challenging problem we need to know the eigenmodes of the covering space. The covering space has the metric

$$ds^2 = dt^2 - R^2(t)d^2; \quad (3.1)$$

where the d^2 is the metric on hyperbolic three-space,

$$d^2 = d^2 + \sinh^2 d^2 + \sin^2 d^2 : \quad (3.2)$$

Perturbations in such a spacetime can be expanded in terms of spherically symmetric solutions of the Helmholtz equation $(+ q^2)Q = 0$, where the Δ is the Laplace operator on H^3 ,

$$Q = \frac{1}{\sinh^2} \frac{\partial}{\partial} \sinh^2 \frac{\partial Q}{\partial} + \frac{1}{\sin^2} \frac{\partial}{\partial} \sin \frac{\partial Q}{\partial} + \frac{1}{\sin^2} \frac{\partial^2 Q}{\partial^2} : \quad (3.3)$$

The eigenfunctions are given by

$$Q^{q,m}(\theta, \phi) = X_q(\theta)Y_m(\phi); \quad (3.4)$$

where the Y_m 's are spherical harmonics and the radial eigenfunctions are given by

$$X_q(\theta) = (-1)^{q+1} \frac{(q^2)}{(q^2 + \theta^2)} q \sinh \theta \frac{d^{q+1} \cos(\frac{p}{q^2 - 1})}{d(\cosh \theta)^{q+1}} : \quad (3.5)$$

The wavenumber, $k = 2$, is related to the eigenvalues of the Laplacian by

$$k^2 = q^2 - 1 : \quad (3.6)$$

In a compact hyperbolic space the eigenmodes will be discrete and the spectrum can be lowered below $k^2 = 0$. Modes with $k^2 < 0$ have no classical interpretation, but can be thought of as describing a form of barrier tunnelling for quantum fluctuations [17].

The physical and comoving counterparts to the wavenumber k and wavelength are scaled such that

$$k_{\text{phys}} = \frac{k}{R(t)}; \quad k_{\text{cmvg}} = \frac{k}{R_0} = kH_0 \frac{p}{1 - \frac{p}{H_0}}; \quad (3.7)$$

Fluctuations in the temperature of the cosmic microwave background are partly due to variations in the gauge invariant gravitational potential (x) on the last scattering surface $x = R_{\text{LSS}}$. The connection between eigenvalue spectra and observed fluctuations in the CMB follows from the relation

$$x = a_{q,m} Q^{q,m}(x); \quad (3.8)$$

The expansion coefficients $a_{q,m}$ are fixed by the primordial power spectrum. Moreover, any physical mechanism for generating that primordial power will be influenced by the shape of the eigenmodes and the eigenspectrum, for no matter how skilled the drummer, a snare drum will not sound like a timpani.

IV. LONG WAVELENGTH MODES

Here we study long wavelength modes in small hyperbolic universes. We do this without explicitly solving for the eigenmodes by exploiting the close connection between eigenvalue spectra and topology. We find a number of useful topological results pertaining to long wavelength modes.

For hyperbolic manifolds of dimension $d \geq 3$ there is a remarkable connection between geometry and topology. The rigidity theorem of Mostow-Patras [18] proves that any connected and orientable manifold of dimension $d \geq 3$ supports at most one hyperbolic metric (up to diffeomorphisms). This means that geometrical quantities such as volume, diameter, injectivity radius, geodesic length spectra and eigenvalue spectra are all topological invariants for compact hyperbolic manifolds.

A compact hyperbolic universe has spatial sections of the form $= H^3$, where the fundamental group, Γ , is a discrete subgroup of $SO(3;1) = PSL(2;C)$ acting freely (i.e. without fixed points) and discontinuously (since it is discrete). According to Poincaré's fundamental polyhedron theorem [19], Γ can be obtained by gluing together

the faces of a polytope in hyperbolic space. The polytope is otherwise referred to as the manifold's fundamental cell or Dirichlet domain².

In this section we will put the topologists' interest in the eigenvalue spectra to good use. Without having to solve for the eigenmodes explicitly we can prove several results concerning the existence of long wavelength modes in compact hyperbolic spaces. In particular, we prove that all known compact hyperbolic spaces admit supercurvature modes. In addition, we show that there exist finite volume, compact hyperbolic manifolds with an arbitrarily large number of modes with arbitrarily long wavelengths. We also observe that the existence of arbitrarily long wavelength modes has not been ruled out for any compact hyperbolic manifold, although equally, there are no results proving that such an example can not be found.

To relate these results to cosmology we need to recall the relationship between curvature, redshift, density and the radius of the last scattering surface (LSS) in a hyperbolic universe. The curvature radius is fixed by the scale factor $R(t)$ since the metric (3.2) has unit curvature radius. The radius of the last scattering surface at redshift z is given by

$$R_{\text{LSS}} = R \operatorname{arccosh} \frac{1 + \frac{2(1 - \rho)}{\rho(1 + z)}}{2} \quad R_{\text{LSS}} : \quad (4.1)$$

The volume of space encompassed by the LSS is

$$V_{\text{LSS}} = R^3 (\sinh(2R_{\text{LSS}}) - 2R_{\text{LSS}}) : \quad (4.2)$$

The radius of the last scattering surface today is approximately equal to the curvature radius if $\rho_0 = 0.5$. If $\rho_0 = 0.4$ we find $R_{\text{LSS}} = 2R_0$; if $\rho_0 = 0.1$ we find $R_{\text{LSS}} = 3.6R_0$. The angle subtended by the curvature scale on the last scattering surface is approximately

$$\operatorname{curv} \frac{1.68 \frac{0}{1}}{\frac{0}{1}} : \quad (4.3)$$

The above expression assumes that the universe has been matter dominated since decoupling. This will be true if matter-radiation equality was reached before decoupling so that

$$z_{\text{eq}} = 24000 \rho h^2 > z_{\text{LSS}} \quad \rho h^2 > 0.052 : \quad (4.4)$$

Assuming $h > 0.5$, (4.3) will be valid so long as $\rho > 0.2$. Since, roughly speaking, the $^{\text{th}}$ multipole moment measures power on angular scales³ of ~ 1 , supercurvature modes produce power on angular scales $\sim \operatorname{curv}$, where

$$\operatorname{curv} \frac{p \frac{1}{0}}{0} : \quad (4.5)$$

In a universe with $\rho_0 = 0.5$, only the $\ell = 2$ quadrupole probes supercurvature modes, while in a universe with $\rho_0 = 0.3$, supercurvature modes contribute to multipoles below $\ell = 6$. This tells us that supercurvature modes are responsible for the large angle power on the last scattering surface.

Using (4.2) we can estimate the redshift when a fundamental cell first dropped within the last scattering surface from the relation

$$1 + z = \frac{2 \left(\frac{1}{0} \frac{1}{1} \right)}{0 \left(\cosh r_+ - 1 \right)} : \quad (4.6)$$

where r_+ is the outradius of the manifold. Taking Thurston's manifold [20] (see Fig. 2) with $\operatorname{Vol}(M_h) = 0.98137$ and $r_+ = 0.748537$ as a particular example, we find that the fundamental cell dropped inside the LSS no earlier than $z = 9.2$ if $\rho_0 = 0.4$. Today there would be approximately 86 copies of the fundamental cell within the LSS (this is the ratio of volume of the optically observable universe to the comoving volume of Thurston's manifold).

Returning to our treatment of the eigenvalues, we introduce the ordering $0 < q_1 < q_2 \dots$, where the eigenvalues are counted with their multiplicities. The mathematical literature is littered with dozens of upper and lower bounds for the q_j 's in terms of the volume, diameter or isoperimetric constant of a manifold. Unfortunately most of these bounds are not very sharp since the results apply to a great variety of manifolds. Sharper bounds can probably be found by restricting ones attention to three dimensional manifolds with constant negative curvature.

Most papers deal with the first eigenvalue, q_1 , whereas we are most interested in eigenmodes with $q^2 \gtrsim 1; 1 + \frac{1}{2}$ where 1. Eigenmodes in this interval correspond to modes with wavelengths $\sim 2 = \pi$. Nevertheless, some of the bounds on q_1 are useful to us.

Many of the bounds on q_1 employ Cheeger's isoperimetric constant [21]. Isoperimetric inequalities relate the volume of a manifold to its surface area. Cheeger's constant is defined to be

$$h_C = \inf_{S \subset M} \frac{\operatorname{Vol}(S)}{\inf_{M \setminus S} \operatorname{Vol}(M_1); \operatorname{Vol}(M_2)} : \quad (4.7)$$

Here S runs through all compact codimension one submanifolds which divide M into two disjoint submanifolds M_1, M_2 with common boundary $S = \partial M_1 = \partial M_2$. A familiar example is the two-sphere. In this case M_1 and M_2 are both hemispheres, $S = \partial M_1$ is a great circle and we find $h_C(S^2) = 1$.

Using his isoperimetric constant, Cheeger [21] derived the lower bound

$$q_1^2 \gtrsim \frac{h_C^2}{4} : \quad (4.8)$$

²A simple analogue in two dimensions is the torus (a rectangle with opposite sides identified) which is $E^2 = \mathbb{R}^2/\Gamma$. Γ is the group generated by a translations by L_x in the x direction, and L_y in the y direction.

³The reasoning being that the $^{\text{th}}$ multipole has 2 zeros in the range $2[\ell; \ell+1]$, with approximately equal spacings of ~ 1 .

A decade later Buser [22] derived the upper bound

$$q_1^2 \leq 4h_c + 10h_c^2 : \quad (4.9)$$

Cheeger's bound is valid for arbitrary closed manifolds in any dimension. Buser provided a general bound valid in any dimension for any closed manifold with bounded Ricci curvature. We have quoted Buser's bound in the form relevant for 3-manifolds with constant negative curvature. Given a 3-manifold, we can in principle calculate Cheeger's constant and subsequently use it to place bounds on q_1 . Recasting Cheeger's inequality in terms of wavelengths we find the maximum wavelength is bounded from above by

$$\max \frac{4}{h_c^2 + 4} : \quad (4.10)$$

Similarly, Buser's inequality provides a lower bound on the maximum wavelength:

$$\max \frac{2}{10h_c^2 + 4h_c - 1} : \quad (4.11)$$

If $h_c > 2$ we would learn that $\max < 1$. That is, there would be a long wavelength cut-off. Similarly, if $h_c > 2 \sqrt{1 + 4^2} = 12.7$ we would learn that $\max < 1$ and therefore no supercurvature modes. On the other hand, an interesting lower bound occurs when $h_c < (\sqrt{14 + 40^2} - 2) = 10 - 1.82$. In this case it is likely that the manifold supports supercurvature modes. We say "likely" since Buser's bound cannot definitively prove there are supercurvature modes. It may be that q_1 lies below 1, i.e. the lowest eigenmode may be a tunnelling solution.

In principle it should be possible to provide a numerical estimate of Cheeger's constant by trying a number of trial partitions. The best partitions could then be varied slightly and the search continued until the optimal partition is found. A judicious choice for the original trial partitions would ensure rapid convergence. The form of Cheeger's constant (4.7) suggests that the trial partitions should employ fairly smooth surfaces S that divide into two approximately equal-sized pieces. At present no numerical algorithm has been written, but it is hoped that the facility will be available in later releases of the SnapPea program [23].

In the absence of numerical results we have to resort to analytic estimates. An upper bound for Cheeger's constant can be derived using geodesic balls [24]:

$$h_c \leq \frac{\partial \ln V(\cdot; x)}{\partial r} : \quad (4.12)$$

Here $V(\cdot; x)$ is the volume of a geodesic ball with radius centred at x . The radius of the ball must be larger than the injectivity radius r_{inj} , but small enough so that $V(\cdot; x) < \text{Vol}(\cdot) = 2$. A lower bound for Cheeger's constant is quoted by Gallot [25]:

$$h_c \leq \frac{4 \frac{p}{j} \frac{p}{j+j} \frac{p}{j-j}}{\text{diam}(\cdot) (\sinh \frac{p}{j+j} + \cosh \frac{p}{j-j})} ; \quad (4.13)$$

where

$$(\text{diam}(\cdot))^2 \quad \text{and} \quad 2 \cdot z : \quad (4.14)$$

Applying these bounds to Thurston's manifold we have $r_{\text{inj}} = 0.289, 1.07$, $\text{diam}(\cdot_{\text{Th}}) = 1.50$ and $\text{Vol}(\cdot_{\text{Th}}) = 0.9814$ so that

$$1.03 \leq h_c(\cdot_{\text{Th}}) \leq 6.42 : \quad (4.15)$$

The softness of these bounds prevent us from saying anything very definite about the allowed wavelengths. The same was found to be true for all the manifolds in the SnapPea census. However, useful bounds based on (4.8) and (4.9) will be possible when Cheeger's constant is available numerically.

Other bounds on q_j exist that do not use Cheeger's constant. Cheng [26] provides the bound

$$q_j^2 \leq 1 + \frac{8(1 + \frac{2}{j})^2}{\text{diam}(\cdot)^2} ; \quad (4.16)$$

and Buser [27] provides the bound

$$q_j^2 \leq 1 + c \frac{j}{\text{Vol}(\cdot)}^{2/3} ; \quad c > 1 ; \quad (4.17)$$

but the constant c is not quoted explicitly. Cheng derived his bound by first proving that the eigenvalues q_j in a closed manifold are always lower than the first eigenvalue of an open geodesic ball with the same curvature and radius $r_0 = \text{diam}(\cdot) = (2j)$.

TABLE I. Scenes from the SnapPea census.

	Vol	r	r_{f}	r_{inj}
m 003 (-3,1)	0.9427	0.5192	0.7525	0.2923
m 003 (-2,3)	0.9814	0.5354	0.7485	0.2890
s556 (-1,1)	1.0156	0.5276	0.7518	0.4157
m 006 (-1,2)	1.2637	0.5502	0.8373	0.2875
m 188 (-1,1)	1.2845	0.5335	0.9002	0.2402
v2030 (1,1)	1.3956	0.5483	1.0361	0.1831
m 015 (4,1)	1.4124	0.5584	0.8941	0.3971
s718 (1,1)	2.2726	0.6837	0.9692	0.1696
m 120 (-6,1)	3.1411	0.7269	1.2252	0.1570
s654 (-3,1)	4.0855	0.7834	1.1918	0.1559
v2833 (2,3)	5.0629	0.7967	1.3322	0.2430
v3509 (4,3)	6.2392	0.9050	1.3013	0.1729

The bound quoted in (4.16) is not very sharp since Cheng considered manifolds with arbitrary curvature. Here we derive a new, sharper bound by specialising to three dimensional manifolds with constant negative curvature. The first eigenvalue of an open geodesic ball of radius r_0 is found by solving the equation $(-\Delta + q^2)Q = 0$ with the boundary conditions

$$\frac{dQ}{dr}(0) = 0; \quad Q(r_0) = 0; \quad (4.18)$$

The eigenfunction with lowest eigenvalue is radial ($\theta = 0$, $m = 0$),

$$Q^{q00}(r) = \frac{\sin(\frac{p}{q^2} \sqrt{1-r^2})}{\frac{p}{q^2} \sqrt{1-r^2} \sinh(p)}; \quad (4.19)$$

and the boundary conditions demand that

$$q^2 = 1 + \frac{r_0^2}{\frac{2}{p}}; \quad (4.20)$$

From this we derive the bound on the eigenvalues of Δ :

$$q_j^2 = 1 + \frac{2j^2}{\text{diam}(r_0)}; \quad (4.21)$$

Translated into a bound on the allowed wavelengths this reads

$$j \leq \frac{\text{diam}(r_0)}{r_0}; \quad (4.22)$$

Applying this bound to Thurston's manifold we discover that

$$\max(\text{diam}(r_0)) = 1.07; \quad (4.23)$$

so Thurston's manifold supports supercurvature modes. Indeed, this is true for all the 3-manifolds in the SnapPea census. The geometrical constants for a selection of SnapPea's manifolds are collected in Table I. The relevance of these quantities to (4.22) comes from the relation

$$2r_+ \leq \text{diam}(r_0) \leq 2r_+; \quad (4.24)$$

Here r_+ is the inradius and r_+ is the outradius (see the appendix for definitions).

It is interesting to note that the length of the shortest geodesic (twice the length of the injectivity radius r_{inj}) does not grow with the volume. Even the largest manifolds in the SnapPea census, with volumes ~ 6 , have geodesics as short as 0.3 in curvature units. This suggests that even relatively large manifolds still make for interesting small universe models.

Having established that generic compact hyperbolic 3-manifolds support supercurvature modes, we have largely answered the question we set out to answer. Even neglecting the integrated Sachs-Wolfe effect, our results

show that compact hyperbolic models are able to support the supercurvature modes required to produce large angle anisotropy on the last scattering surface. Moreover, we can supplement this result using a theorem due to Buser [28] which states that there exist finite volume compact hyperbolic 3-manifolds with an arbitrarily large number of modes with arbitrarily long wavelength. This theorem proves that any attempt to exclude all compact hyperbolic models on the basis of a lack of long wavelength power is doomed to failure. Admittedly, the manifolds considered by Buser have large diameters, but they also have small injectivity radii so they describe models that are multi-connected on scales smaller than the curvature scale. The fundamental cells for these manifolds are highly anisotropic, which may bring them into conflict with observations, but this is not certain since the face identifications tend to permute all three spatial directions and thus apparent isotropy can be restored.

V. HORNED TOPOLOGIES

In this section we digress to consider a particular class of models that can be partially constrained by COBE data. In Ref. [10], Levin et al. describe them in a universe with the topology of a hyperbolic toroidal horn. The topology they consider is the three dimensional analog of the two dimensional pseudosphere. The pseudosphere, referred to as a cusp by mathematicians, is topologically equivalent to $S^1 \times [0; 1)$, where S^1 is a circle. Figure 1 shows a portion of the pseudosphere embedded in three dimensional space. The pseudosphere is described in the upper half plane representation of H^2 by

$$ds^2 = \frac{dx^2 + dz^2}{z^2}; \quad (5.1)$$

with the identifications $x = x + nL_x$ with $n \in \mathbb{Z}$.

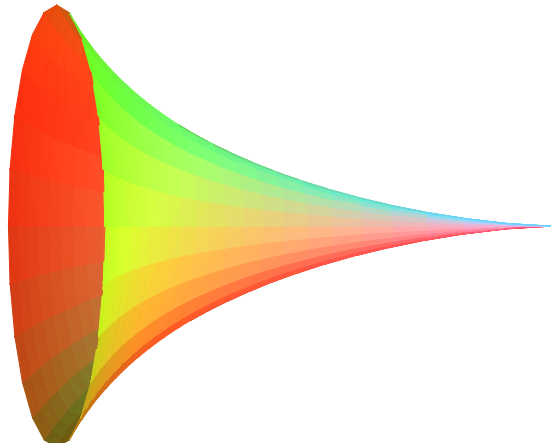


FIG. 1. A portion of the pseudosphere.

Cusps in d dimensions are analogously defined to be of the form $E^{d-1} \times [0; 1)$ where E^{d-1} is a $d-1$ at topology in $d-1$ dimensions. It should be emphasised that the line $z = \text{const.}$ connecting x and $x + L$ is not a geodesic. Geodesics in the upper half plane model appear as half-circles of the form $x^2 + z^2 = a^2$, perpendicular to the boundary plane.

The hyperbolic horn studied in Ref. [10] is of the form $T^2 \times [0; 1)$ where T^2 is the two-torus. In the upper half plane model of H^3 ,

$$ds^2 = \frac{dx^2 + dy^2 + dz^2}{z^2}; \quad (5.2)$$

the horn is defined by making the identifications $x = x + nL_x$ and $y = y + mL_y$. Since the fundamental group of the hyperbolic horn is abelian, geodesics on the horn are non-chaotic. This means that the horn's eigenmodes can be written down explicitly.

The calculational simplicity of the horn model is offset by some unappealing physical characteristics. Not only is the horn noncompact and infinite in volume, but it also suffers from severe global anisotropy. The anisotropy can be seen by moving to spherical coordinates centred at $(x; y; z) = (0; 0; 1)$. Our ghost images then appear at the points

$$\begin{aligned} &= \operatorname{arcsinh} \operatorname{arccosh} \sqrt{1 + \frac{1}{2}(n^2 L_x^2 + m^2 L_y^2)}; \\ &= \arccos \frac{1 + \frac{4}{(n^2 L_x^2 + m^2 L_y^2)}}{0 \quad 1}^{1=2}; \\ &= \arcsin \theta \sqrt{\frac{m L_y}{n^2 L_x^2 + m^2 L_y^2}}; \end{aligned} \quad (5.3)$$

The ghost images are evenly distributed in the direction, but distant images pile up along the axis of the horn ($\theta = \pi/2$).

Because the horn's fundamental group is abelian, there will be a long wavelength cut-off in directions orthogonal to the axis of the horn. In this respect the hyperbolic horn is similar to the flat topology $= R \times T^2$. The difference is that the torus cross-sections of the horn do not have fixed area. As we move away from the origin, the torus area decreases like

$$A(T^2) = \frac{1}{2} L_x L_y \exp(-2 \sinh \theta); \quad (5.4)$$

This means that the wavelength cut-off gets shorter and shorter as we move toward the cusp. Moreover, the decrease is doubly exponential with increasing proper distance. This has the effect of suppressing all temperature fluctuations in the direction of the horn, leading to a "hot-spot" [10] in the microwave sky.

Considering that there are an infinite number of hyperbolic three manifolds to choose from, it might seem strange to focus on one particular example. However, it

turns out that many manifolds have horn-like regions. To see why one needs to understand something about how hyperbolic three manifolds are constructed. According to Jørgensen's theorem [29], all finite volume hyperbolic three manifolds can be obtained by Dehn surgery on a finite number of link components in S^3 . A link component is constructed by drilling out a solid tubular knot or link from spherical space. The complement of this link (i.e. the space outside the link) will almost always be topologically equivalent to a hyperbolic three manifold with one or more cusps. If one happened to live deep inside a cusp, the universe would look exactly like a toroidal horn.

While the finite volume of the cusped manifolds makes them more appealing than the basic hyperbolic horn, they are still non-compact. In order to arrive at compact models we need to perform Dehn surgery on the link. The surgery involves cutting out a portion of the link and replacing it with a solid torus that is first twisted around the link in some non-trivial way. Without going into details, it is sufficient to note that the twisting can be parametrised by two integers $(p; q)$. In the limit $p; q \neq 1$ with $p; q$ relatively prime, the original cusped manifold is recovered. For small $p; q$ the cusp can be completely removed. For large values of $p; q$ the end of the cusp is rounded off leaving a "horned manifold". If one happened to live deep inside one of the horns, the universe would look similar to how it does in the infinite toroidal horn. The exact correspondence is broken since Dehn surgery makes the fundamental group non-abelian. This means that the geodesics will be chaotic and the eigenmodes complicated. Nonetheless, for high order Dehn fillings the chaos should be mild and it seems reasonable to expect a hot spot in the CMB if one lived in a horned region of the manifold.

The preceding considerations have shown that the results of Ref. [10] apply in certain regions of a large class of three manifolds. If we happened to live in one of these horned regions, we would see a severe suppression of CMB fluctuations along the horn. Levin et al. found that this effect was not masked by the integrated Sachs-Wolfe effect, so the COBE satellite would have detected hot spots in the CMB. However, the absence of hot spots is not a very strong constraint on us living in a cusped manifold. This is because cusps only account for a very small portion of a cusped manifold's volume. Therefore, it is very unlikely that we would be living in or near a cusp. If we make what topologists refer to as a "thick-thin" decomposition, we find that most of a manifold's volume is in the "fat" part and very little is in "thin" regions such as cusps. The chance that we live deep inside a cusp is even smaller since the volume of a cusp decreases as $\exp(-2e)$, where e is the proper distance down the cusp. We are far more likely to live in a "fat" portion of a manifold where the breaking of global isotropy is much less noticeable.

In summary, it would be surprising if we did live in a horned region, and the results of Levin et al. con-

that we do not!

VIM METHOD OF IMAGES

We now return to the problem of modelling CMB fluctuations in a compact hyperbolic universe. Any function defined on the compact space $= H^3 =$ must be invariant under the action of the fundamental group

$SO(3;1)$. The simplest way to enforce this condition employs the method of images:

$$Q(x) = \sum_{g \in G} Q(gx); \quad (6.1)$$

The same method can be used to generate any n -point function in the compact space via a sum over translated copies of the corresponding function in the covering space. In a recent paper, Bond et al [30] applied the method of images to the two-point correlation function in several compact hyperbolic universes.

The simplicity of the method of images is marred by the severe divergences encountered in the sum over images. The number of images proliferate as their distance from the original increases. In Euclidean or spherical space this proliferation is sub-exponential and the divergence of the sum can be controlled using a simple regulariser [31]. In hyperbolic space the number of images grows exponentially with distance and the sum over images diverges for any real wavenumber k , no matter what regulariser is used.

In the last few years a resummation formula [15,16] has been developed that allows the sum over images to be truncated after a finite number of images. Using this resummation method the divergence in the sum over images can be avoided.

Before describing the resummation procedure we must sound some cautionary notes.

The divergence of the sum over images clearly presents a technical problem in calculating eigenfunctions or eigenvalues of the Laplace-Beltrami operator, or n -point correlation functions. Whether or not this is a physical problem is less clear. We have heretofore assumed implicitly that the entire sum over images contains physical information. However, although the standard method of

Bond et al have not yet published details of how they implemented the method of images. Consequently, the following section is not intended to be a critique of their work, but rather a general discussion of the difficulties inherent in implementing the method of images. Indeed we thank them for stressing to us the potential power of the method of images in addressing these problems, and eagerly anticipate a more lengthy publication which includes details of their treatment of the divergence of the sum.

expanding the fluctuation spectrum in the static eigenmodes requires that we perform the full sum, causality ensures that there cannot be any information coming from beyond the causal horizon. Thus the physical problem should be just as well described by retarded Green's functions of the metric and underlying matter fields. These have the advantage of incorporating the causal horizon as a physical cut-off and should truncate the method-of-images sum. Our technical problems are not necessarily solved in practice for the number of images can still be extremely large (in compact hyperbolic inflationary models the causal horizon is typically at a distance of more than 16 times the curvature scale [3]), and the number of images grows exponentially with this distance. One must still therefore sum over a very large, albeit finite, number of images in calculating the Green's functions. We will address this approach in upcoming publications.

Another physical complication is that the last scattering surface is actually a thick spherical shell. Observations of the CMB temperature in a particular direction are radial averages of the temperature through this shell. This poses a potential problem. In the manifolds of trivial topology, spherical symmetry means that the eigenmodes of the Laplace-Beltrami operator can be chosen to be separable functions of radius and angle, with each resulting radial eigenfunction carrying power in a narrow range of radial frequencies. Not so in the generic hyperbolic manifold, where the boundary conditions violate the spherical symmetry, and the fundamental groups are non-abelian. This implies some correlation between long-distance and short-distance power. If low k modes have significant small scale structure, so that a mode has several zero-crossings over the thickness of the last scattering surface, then the long-range correlations inherent in the low k modes, will be suppressed by the radial averaging over the LSS. Understanding the small-distance structure of the low- k modes is therefore essential. Since this small scale structure will be generated by the most distant images, one must correctly perform the full method-of-images sum, or at least its causal part.

Having burdened the reader with the limitations inherent in this approach, we are now ready to describe the resummation method for the sum over images. First we must introduce some additional machinery. To keep the presentation accessible we will illustrate the concepts using a particular hyperbolic 3-manifold first discovered by Thurston [20]. A glossary of unfamiliar mathematical terms is compiled in the appendix.

Hyperbolic 3-space can be viewed as the unit hyperboloid (mass-shell)

$$x_0^2 + x_1^2 + x_2^2 + x_3^2 = 1; \quad (6.2)$$

embedded in 4-dimensional Minkowski space. We can relate this representation to the induced metric on H^3 , (3.2), by the coordinate identifications

$$x_0 = \cosh \phi; \quad x_1 = \sinh \phi \cos \theta; \quad$$

$$x_2 = \sinh \sin \cos ; \quad x_3 = \sinh \sin \sin : \quad (6.3)$$

From this perspective it is easy to understand why the isometries of H^3 are described by the orientation preserving homogeneous Lorentz group in 4-dimensions, $SO(3;1)$. Given a set of generators a_1, \dots, a_g , any element of the fundamental group can be written as

$$g = \prod_i a_i^{j_i} \quad (i; j_i; m_i \in \mathbb{Z}) ; \quad (6.4)$$

with possible repetitions of the generators. The group element g is called a word, and the length of the word is defined to be

$$l_g = \sum_i j_i : \quad (6.5)$$

Not all words generated according to (6.4) will be unique since the generators are typically subject to a set of relations, e.g. $a_1 a_2 a_1 a_2 = 1$. The number of distinct words with lengths less than or equal to l is denoted $N(l)$. A theorem due to Milnor [32] tells us that $N(l)$ grows exponentially with l if Γ is the fundamental group of a compact hyperbolic manifold. It is precisely this exponential growth that causes problems with the sum over images.

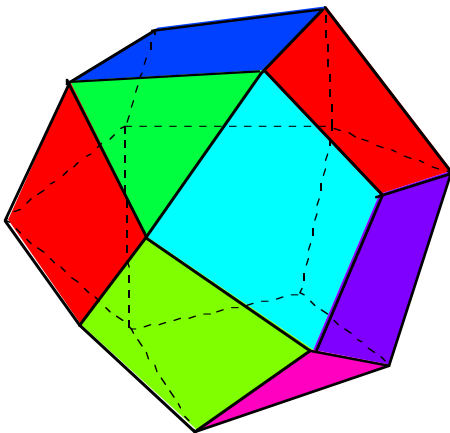


FIG. 2. The fundamental cell for Thurston's manifold.

To illustrate the preceding discussion we use SnapPea [23] to study Thurston's manifold, Γ_h (m 003 (-2,3) in the SnapPea census). The fundamental group, $\Gamma = \pi_1(\Gamma_h)$, has the presentation^{yy}

$$= fa; b : a^2ba^{-1}b^3a^{-1}b; ababa^{-1}b^{-1}ab^{-1}a^{-1}bg : \quad (6.6)$$

The generators of the fundamental group describe identifications in the faces of the fundamental cell shown in Fig. 2.

Thurston's manifold has volume 0.98137, symmetry group $G = \text{fu}; v : u^2; v^2; uvuv = z_2 \cdot z_2$, first homology group \mathbb{Z}_5 and betti numbers $b_0 = b_3 = 1$, $b_1 = b_2 = 0$. The symmetry group describes the symmetries of the manifold. The (rst) homology group [33] is the abelianised version of the fundamental group (6.6). When abelianised, the relations obeyed by the fundamental group collapse down:

$$\begin{aligned} a^2ba^{-1}b^3a^{-1}b = 1 \quad) \quad b^5 = 1 \\ ababa^{-1}b^{-1}ab^{-1}a^{-1}b = 1 \quad) \quad a = b^{-1} ; \end{aligned} \quad (6.7)$$

leaving the homology group

$$H_1(\Gamma_h) = fb : b^5 = 1g = \mathbb{Z}_5 : \quad (6.8)$$

Choosing a coordinate system centred at a maximum of the injectivity radius function [23], the generators have the $SO(3;1)$ matrix representations

$$a = \begin{pmatrix} 0 & 1.4498 & 0.3191 & 0.8911 & 0.4538 \\ 0 & 0.5653 & 0.5653 & 0.8911 & 0.4538 \\ 0 & 0.8844 & 0.8844 & 0.8911 & 0.4538 \\ 0 & 0.0000 & 0.0000 & 0.4538 & 0.8911 \end{pmatrix}^A ; \quad (6.9)$$

and

$$b = \begin{pmatrix} 0 & 2.9351 & 2.4389 & 1.1390 & 0.6073 \\ 0 & 0.9195 & 0.4233 & 1.1390 & 0.6073 \\ 0 & 2.5987 & 2.5987 & 0.8587 & 0.5125 \\ 0 & 0.1255 & 0.1255 & 0.5125 & 0.8587 \end{pmatrix}^B : \quad (6.10)$$

The image of any point $x \in H^3$ can now be found by matrix multiplication. To give an example, the origin $x = 0$ has $\Gamma = 0$ and corresponds to the point $[1; 0; 0; 0]$ when embedded in four dimensional Minkowski space. Acting on this point by a takes it to the point $[1.450; 0.565; 0.884; 0]$. This point has $\Gamma = 0.9161$, $\Gamma = 2.1395$ and $\Gamma = 0.0157$, and so lies a distance 0.9161 units away in 3-space.

Points lying on a symmetry axis of a group element will be translated the shortest distances. Conversely, the further a point lies from the symmetry axis of a group element, the further it is translated by that element. Since the fundamental group acts differently on different points, compact hyperbolic models are not homogeneous. Nor are they isotropic since there are preferred symmetry axes. Points on the symmetry axis of a group element can be located by finding the eigenvectors of the $SO(3;1)$ matrix describing the group element. The two real eigenvectors define points on the lightcone enclosing the hyperboloid (6.2). The line passing through these two points defines the symmetry axis of the group element. The intersection of this line with the hyperboloid (6.2) defines the point in H^3 that is translated the shortest distance. For example, a has the two real eigenvectors

$$\begin{aligned} e_1 &= [0.7491; 0.3497; 0.6563; 0.0896] ; \\ e_2 &= [0.7350; 0.2687; 0.6460; 0.2252] ; \end{aligned} \quad (6.11)$$

^{yy}A presentation lists the group generators followed by any words which are equivalent to the identity.

and the line they define in Minkowski space intersects the hyperboloid at the point

$$v = [1.2428; 0.2409; 0.6425; 0.2716]; \quad (6.12)$$

Acting on this point by α leads to the image point

$$v_a = [1.0292; 0.1431; 0.19035; 0.0496]; \quad (6.13)$$

a distance²² 0.8894 units away in 3-space.

By acting on points lying on the symmetry axis of each group element it is possible to compile a list of the minimal geodesics. A typical isometry is a corkscrew type motion, consisting of a translation of length L along a geodesic, combined with a simultaneous rotation through an angle θ about the same geodesic. The length and torsion can be found directly from the eigenvalues of the group element, and are conveniently listed by the SnapPea program [23]. Table II records both the length and the torsion of all geodesics with $L < 2$.

Each word g^2 does not necessarily produce a unique minimal geodesic. The minimal geodesic generated by ab^2 has the same length and torsion as that generated by b . The mapping between words and minimal geodesics is many to one. To make the mapping one to one, the words need to be grouped into conjugacy classes. Two words, g and g^0 belong to the same conjugacy class if and only if they are equal up to an isometry²³:

$$g \cdot g^0 \cdot i \cdot g^0 = f^{-1} g f \quad (f^2) : \quad (6.14)$$

A theorem by McLean [34] then states that there is a one to one correspondence between conjugacy classes of the fundamental group and the periodic geodesics. If we define \mathcal{P} to be the set of all geodesic loops at some point p , endowed with the product $a \cdot b$ (rst b then a) for all $a, b \in \mathcal{P}$, then \mathcal{P} is isomorphic to $\pi_1(\mathcal{M})$.

TABLE II. Minimal geodesics shorter than 2

Length	Torsion	Word
0.57808244	2.13243064	ab
0.72156837	-1.15121299	b
0.889442997	2.94185905	a
0.998325189	-2.92101779	ab^1
1.040315125	0.98237189	aba^1b
1.793800843	-1.55687105	a^2b
1.822279900	-2.41353903	ab^1a^1b

²²A simple way to work out the length of the shortest geodesic connecting two points is to first perform an $O(3;1)$ rotation of the coordinate system so that one of the points lies at the origin of H^3 . The proper distance between the two points is then found by taking the arccosh of the other point's "time" coordinate, in accordance with (6.3).

²³e.g. $ab^2 \cdot bab \cdot ababa^1 = b^1 aba^1 b \cdot aba^1 b$

This link between geodesic loops and the fundamental group can be used to re-express the sum over images (6.1) as a sum over periodic orbits. The exponential growth in the number of words with symbolic lengths l_g is echoed by the exponential growth in the number of closed geodesics with physical lengths L :

$$N(L) \sim \frac{e^{hL}}{hL}; \quad (6.15)$$

where h is the Kolmogorov-Sinai entropy of the geodesic flow [35]. It is interesting to note that $h / V \approx 1$ while H / V is larger. This is because the Kolmogorov-Sinai entropy measures the rate of mixing and smaller manifolds mix better, while H measures the complexity of the fundamental group, and larger manifolds have more complicated topologies [36].

A. The Gutzwiller Trace Formula

By mapping the sum over images to a sum over periodic orbits we are able to co-opt techniques developed to tackle quantum chaos. The connection between quantum eigenvalues and classical periodic orbits was first pointed out by Gutzwiller [14]. The Gutzwiller trace formula expresses the density of states of a chaotic system in terms of a sum over its classical periodic orbits. Like the sum over images introduced earlier, Gutzwiller's sum is not absolutely convergent for any real wavenumber. This is to be expected since we have simply mapped one divergent sum into another.

If we introduce the spectral function $\langle q \rangle$, so that eigenvalues of the operator $-\nabla^2 + q^2$ are given by the condition $\langle q \rangle = 0$, then Gutzwiller's trace formula takes the form

$$\langle q \rangle = e^{i \pi n} \sum_p \frac{1}{2} \exp(iS_p) i_p \sum_j \frac{1}{2} + j u_p; \quad (6.16)$$

where p denotes a primitive periodic orbit, S_p its action, i_p its phase and u_p its instability exponent [16]. The periodic orbits have been separated into primitives, p , and repeats of primitives, $(p)^j$. Primitive orbits are like prime numbers, they cannot be formed from any product of shorter orbits. The phase factor $\exp(i \pi n)$ introduces the mean wavenumber staircase, $n(q)$, which is a smoothed version of the integrated level density $n(q)$, that counts the number of eigenmodes with eigenvalues less than or equal to q . The smoothing is accomplished by averaging $n(q)$ over a range in q comparable to the mean eigenvalue spacing. We observe that the spectral function (6.16) is closely related to Feynman's path integral.

The products in (6.16) are converted into sums using the Euler identity [15] leading to an expression of the form

$$X(q) = c \exp(i n(q) + i s(q)); \quad (6.17)$$

where X labels pseudo-orbits formed from linear combinations of periodic orbits, according to their lengths $L_p = m_p L_p$. The action of a pseudo orbit is the sum of the actions of its constituent periodic orbits, $S_p = m_p S_p$. The amplitude, c , is controlled by the phases and instability exponents of the orbits used to build the pseudo orbit [16]. The general expression for c is very complicated, but for large m_p it takes the asymptotic form

$$c \underset{p}{\sim} (1)^{m_p} \exp\left(\frac{1}{2} m_p^2 u_p L_p\right) m_p ! \quad 1 : \quad (6.18)$$

Thus the most important pseudo-orbits are composed of relatively stable, short primitive orbits that are only traversed once. This is exactly what we would expect from a Feynman path integral perspective.

The sum over pseudo-orbits in (6.17) diverges since the number of pseudo-orbits also increases exponentially with increasing length. However, Berry & Keating [15] showed that the sum in (6.17) can be truncated after a finite number of pseudo-orbits. Heuristically this is because the Gutzwiller trace formula imposes strong correlations between the longest orbits and the shortest orbits. This implies that for each q there is a symmetry point about which the sum can be divided into a "head" and "tail". Remarkably, the divergent tail can be resummed to produce a new series that reproduces the head, term by term [15]. Consequently, the spectral function can be truncated:

$$X(q) = \sum_{L \leq L(q)} c \exp(i n(q) + i s(q)); \quad (6.19)$$

where the the maximum length pseudo-orbit, $L(q)$, has action $S(q)$ given by

$$\frac{d}{dq} (S(q) - n(q)) = 0; \quad (6.20)$$

A similar resummation procedure can be used to derive an expression for the eigenmodes as a sum over the short periodic orbits [16].

We now have most of the tools in hand to explicitly derive the eigenvalues and eigenmodes of a compact hyperbolic manifold. The lowest eigenvalues are still difficult to compute since we only know the counting function $n(q)$ asymptotically for large q in the form of Weyl's asymptotic formula [37]:

$$n(q) = \frac{\text{Vol}(\mathcal{M})}{3} q^3 + O(q^2); \quad (6.21)$$

Using SnapPea we can obtain a listing of all the pseudo-orbits with lengths less than about 6. The action of each pseudo-orbit is directly proportional to its length since

the covering space is homogeneous and isotropic. Similarly, the divergence of nearby orbits is uniform throughout phase space and their phase difference is negligible, so the amplitude c will depend only on the length of the pseudo-orbit. With a more precise expression for the smoothed counting function $n(q)$ we could use the SnapPea census to derive the eigenvalue spectra for several hundred small volume, compact hyperbolic manifolds. The size of the sample suggests that this approach would yield a fair understanding of what features are generic to the eigenvalue spectra of compact hyperbolic manifolds. However, without better control over the smoothed counting function we are unable to directly calculate low-lying eigenvalues. This is unfortunate since it is these long wavelength modes that we are most interested in when calculating large angle fluctuations on the last scattering surface. We hope to return to this question in a future publication.

For now we will restrict ourselves to some general observations based on SnapPea's listing of the short minimal geodesics. Typical closed geodesics, such as those listed in Table II for Thurston's manifold, involve a considerable torsion. A similar twisting occurs in 5 of the 6 compact, orientable at three manifolds [38]. One example is T_1^3 , where opposite faces of a cube are identified, with one pair of faces identified after a twist through π . If the cube has side length L , then the twisted minimal geodesic has length L and torsion π . As a consequence of this torsion, the lowest eigenmode along the twisted direction must wrap twice around T_1^3 before closing. The maximum allowed wavelength is thus $2L$, not L . We may anticipate a similar phenomenon occurring in hyperbolic space. The shortest geodesic listed in Table II has torsion $2:132431 \approx 2.9465$. This geodesic approximately closes after 3 turns, but may never close exactly if it is an irrational multiple of 2π . Using this Bohr-Sommerfeld style reasoning, it appears likely that compact hyperbolic manifolds will admit very long wavelength modes.

VII. CONCLUSIONS

A hyperbolic drum produces a rich and complex sound. A compact hyperbolic universe is likewise more complex than its spherical or Euclidean counterparts. The simple methods used to constrain models do not work when space is negatively curved. The eigenmodes in a compact hyperbolic space can only be calculated using sophisticated methods derived from number theory. Moreover, hyperbolic models do not suffer the sort of long wavelength cutoff used to exclude toroidal models.

In addition to the issue of what fluctuations are supported on the last scattering surface, there is also the issue of what exactly it was that COBE measured. In a compact hyperbolic universe the curvature radius provides a natural length scale, $R_0 = H_0^{-1} = \sqrt{\frac{P}{\Lambda}}$. The curvature radius sets the length scale where we might

hope to find the first evidence that we live in a multiply connected universe. The curvature radius also sets the angular scale beyond which fluctuations in the cosmic microwave background radiation no longer originate from the last scattering surface. This convergence of physical scales is very unfortunate for COBE since it means that the ISW effect takes over just when things get interesting. Fortunately the next generation of CMB satellites will be able to probe much smaller angular scales, so the ISW effect will not obscure their view of the large scale topology of the universe.

The search for multi-connectedness in our universe is not over. It has barely begun.

V III. ACKNOWLEDGEMENTS

We are indebted to Jeff Weeks for his extensive expert advice on topology and the workings of SnapPea. Our knowledge of cusped manifolds was greatly enhanced by discussions with Bill Thurston and Jeff Weeks. We thank the topologists Bob Brooks, Pat Callahan, Ruth Kellerhals and Alan Reid for sharing their knowledge on the eigenvalue spectra. We have also enjoyed informative discussions with Dick Bond, Andrew Chamblin, Fay Dowker, Gary Gibbons and Janna Levin. N. Cornish was supported by PPARC grant GR/L21488. D. Spergel was supported by the NASA grant for the Microwave Anisotropy Probe. G. Starkman was supported by an NSF career grant.

APPENDIX

The following glossary of terms describes the basic mathematical quantities used in our discussion of topology. Our definitions are designed to be more pictorial than the usual formal definitions found in the mathematical literature.

Diameter: The diameter, $\text{diam } M$, of a manifold M is the greatest distance between any two points on the manifold.

Injectivity radius of a point: The injectivity radius of a point $p \in M$, $r_{\text{inj}}(p)$, is the radius of the largest coordinate chart that can be centered at p . Since a coordinate chart breaks down when any geodesic refocuses, the injectivity radius of a point is half the length of the shortest geodesic connecting p to itself.

Injectivity radius: The injectivity radius of a manifold, $r_{\text{inj}}(M)$, is the smallest injectivity radius of any point in the manifold, ie.

$$r_{\text{inj}}(M) = \inf_{p \in M} r_{\text{inj}}(p) : \quad (8.1)$$

Thus, $r_{\text{inj}}(M) = l_{\text{min}}/2$, where l_{min} is the length of the shortest geodesic in $(M; g)$.

Inradius: The inradius, r , is the radius of the largest

simply connected geodesic ball in $(M; g)$. In other words, r is the largest distance any point in the manifold can be from its closest image. For a compact hyperbolic manifold, the inradius fixes the size of the largest hyperbolic ball that can be placed inside the fundamental cell.

Outradius: The outradius, r_+ , of a compact hyperbolic manifold fixes the size of the smallest hyperbolic ball that can be used to enclose the fundamental cell.

Betti numbers: The zeroth betti number, b_0 , counts the number of disconnected regions in a manifold. The first betti number, b_1 , counts the number of incontractible loops. The second betti number, b_2 , counts the number of incontractible surfaces. Higher betti numbers are similarly defined. The first betti number is equal to the rank of the free abelian part of the first homology group $H_1(\cdot)$. In other words, the first betti number is equal to the number of generators of $H_1(\cdot)$ that are not subject to any relations save those that make the group abelian. Poincaré duality relates the various betti numbers so that in d -dimensions $b_i = b_{(d-i)}$.

Codimension: The codimension is a complementary dimension. A n -dimensional hypersurface living in a d -dimensional space has codimension $d - n$.

- [1] M. Kac, Amer. Math. Monthly 73, (1966).
- [2] For a review see M. Lachieze-Rey and J-P. Luminet, Phys. Rep. 254, 135 (1995).
- [3] N.J. Cornish, D. Spergel & G. Starkman, Phys. Rev. Lett. 77, 215 (1996).
- [4] N.J. Cornish, D. Spergel & G. Starkman, "Circles in the Sky: Finding Topology with the Microwave Background Radiation," gr-qc/9602039.
- [5] C. L. Bennett et al., Astrophys. J. 464, L1, (1996).
- [6] I.Y. Sokolov, JETP Lett. 57, 617 (1993).
- [7] A.A. Starobinsky, JETP Lett. 57, 622 (1993).
- [8] D. Stevens, D. Scott & J. Silk, Phys. Rev. Lett. 71, 20 (1993);
- [9] A. de Oliveira Costa & G.F. Smoot, Ap.J. 448, 477 (1995); A. de Oliveira Costa, G.F. Smoot & A.A. Starobinsky Ap. J. 468, 457 (1996).
- [10] J.J. Levin, J.D. Barrow, E.F. Bunn & J. Silk, Phys. Rev. Lett. 79, 974 (1997).
- [11] M. Kamionkowski & D. Spergel, ApJ. 432, 7 (1994).
- [12] J.R. Gott III, MNRAS 193, 153 (1980); R. Lehoucq, M. Lachieze-Rey, & J-P. Luminet, A&A 313, 339 (1996). B.F. Roukema & A.C. Edge, astro-ph/9706166, submitted to MNRAS.
- [13] W. P. Thurston, Private Communication.
- [14] M.C. Gutzwiler, J. Math. Phys. 11, 1791 (1970); ibid 12, 343 (1971).
- [15] M.V. Berry & J.P. Keating, J. Phys. A 23, 4839 (1990).
- [16] O. Agam & S. Fishman, J. Phys. A 26, 2113 (1993).
- [17] U. Moschella & R. Schaefer, preprint gr-qc/9707007, (1997).

[18] G D . M ostow , *Ann.M ath. Studies* 78 (Princeton University Press, Princeton, 1973); G . P rasad, *Invent.M ath.* 21, 255 (1973).

[19] J. Ratcliffe, *Foundations of Hyperbolic Manifolds*, Graduate texts in Math.149, (Springer-Verlag, Berlin 1994).

[20] W . P . Thurston, *Bull.Am .M ath.Soc.* 6, 357 (1982).

[21] J. Cheeger, in *Problems in Analysis, A symposium in honour of S. Bochner*, (Princeton University Press, Princeton 1970).

[22] P .B user, *Ann .scient .Ec .Norm .Sup.* 15, 213 (1982).

[23] J. Weeks, *SnapPea: A computer program for creating and studying hyperbolic 3-manifolds*, available at <http://www.geom.umn.edu:80/software>.

[24] R .Brooks, in *Topology '90*, eds. B .Apanasov, W .D .Neumann, A .W .Reid & L .Siebenmann, Ohio State University Mathematical Research Institute Publications 1, 61 (1992).

[25] S .G allot, *C .R .Acad .Sc .Paris*, 296, 333 (1983).

[26] S .-Y .C heng, *M ath .Z .* 143, 289 (1975).

[27] P .B user, *M ath .Z .* 165, 107 (1977).

[28] P .B user, in *Geometry of the Laplace Operator*, Proc. Symp .Pure M ath .XX X V I, Am .M ath .Soc . (1980).

[29] W . P . Thurston, *The Geometry and Topology of Three Manifolds*, Lecture Notes, (1979).

[30] J.R .Bond, D .Pogosyan and T .Souradeep, preprint astro-ph/9702212, (1997).

[31] A .Voros, *Commun .M ath .Phys .* 110, 439 (1987).

[32] J.M ilnor, *J .D i .G eom .* 2, 1 (1968).

[33] M .N akahara, *Geometry, Topology and Physics*, (Adam Hilger, Bristol 1990), pg. 113.

[34] H .P .M cKean, *Comm .Pure Appl M ath .* 25, 225 (1972).

[35] N .L .B alazs and A .Voros, *Phys .Rep .* 143, 109 (1986).

[36] S .V .M atveev and A .T .Fomenko, *Russian M ath .Surveys*, 43:1, 3 (1988).

[37] P .H .B erard, *Spectral Geometry: Direct and Inverse Problems*, Lecture Notes in mathematics, 1207, (Springer-Verlag, Berlin 1980).

[38] J. W olf, *Spaces of constant curvature*, (Publish or Perish Inc., W imington, 1984).